U.S. Department of the Interior
U.S. Geological Survey

Characteristics of Fractures in Crystalline Bedrock Determined by Surface and Borehole Geophysical Surveys, Eastern Surplus Superfund Site, Meddybemps, Maine

By BRUCE P. HANSEN, JANET RADWAY STONE, and JOHN W. LANE, JR.

Water-Resources Investigations Report 99-4050

Prepared in cooperation with the
U.S. ENVIRONMENTAL PROTECTION AGENCY, REGION 1

Northborough, Massachusetts
1999

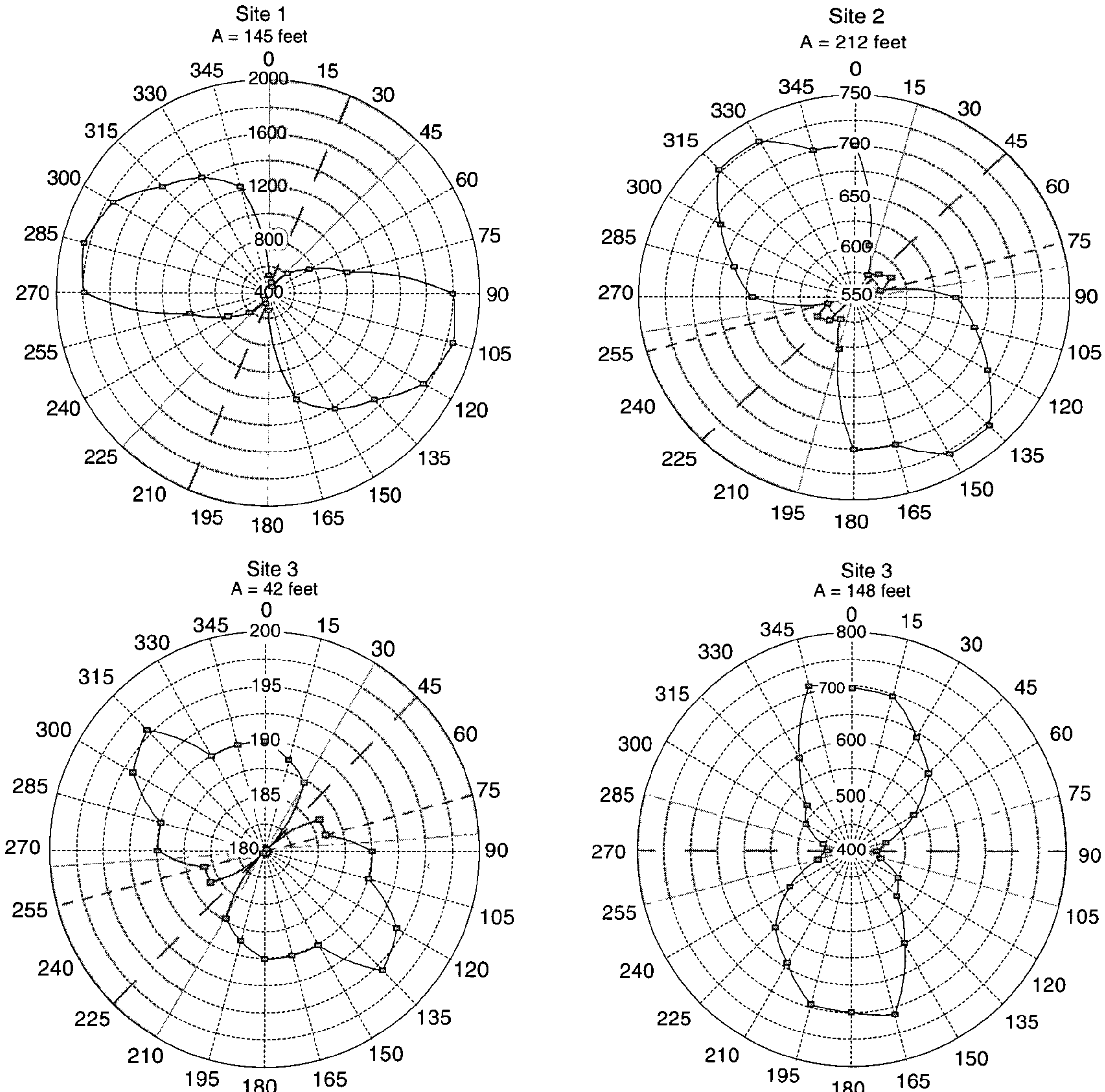

EXPLANATION

○	LINE OF APPARENT RESISTIVITY, IN OHMS-METERS
— —	INTERPRETED PRIMARY FRACTURE STRIKE--Shaded area shows probable range of fracture strike
- - - -	INTERPRETED SECONDARY FRACTURE STRIKE
—▫—	DATA POINTS SHOWING CALCULATED APPARENT RESISTIVITY AT INDICATED AZIMUTHAL DIRECTIONS AND SQUARE-ARRAY SPACING
A	LENGTH OF SIDE OF SQUARE-ARRAY

Figure 4. Azimuthal plots of apparent resistivity and strike of high-angle fractures interpreted from square-array surveys at sites 1–3, Eastern Surplus Superfund Site, Meddybemps, Maine.

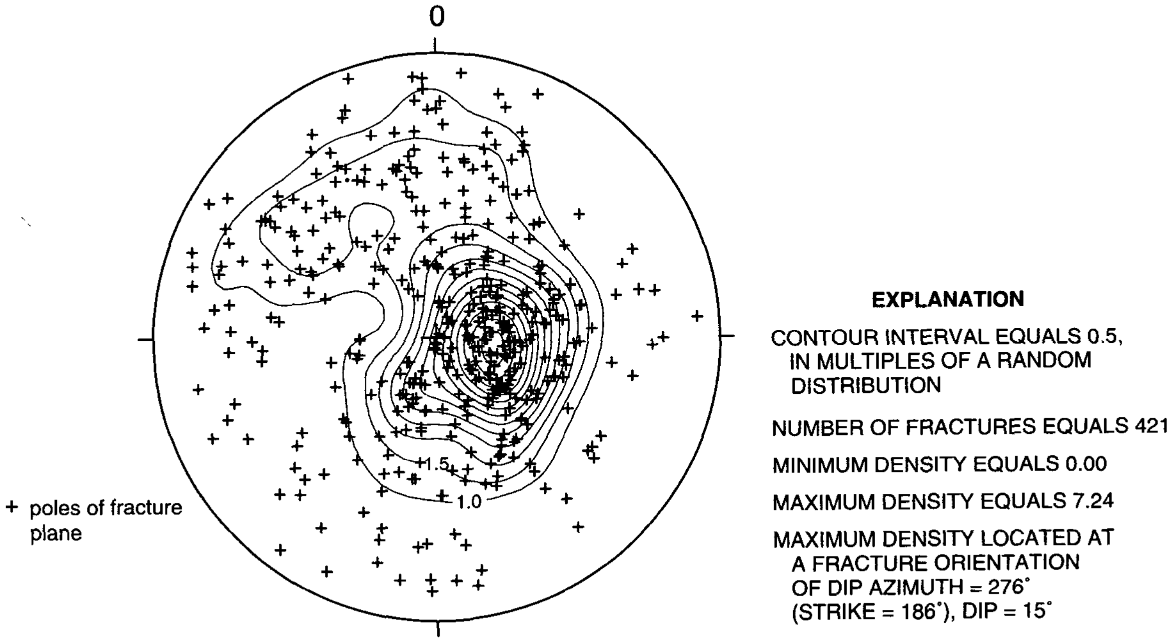

Lower-hemisphere, equal-area stereonet plot of poles to fracture planes and contour plot of relative orientation distribution density of fractures.

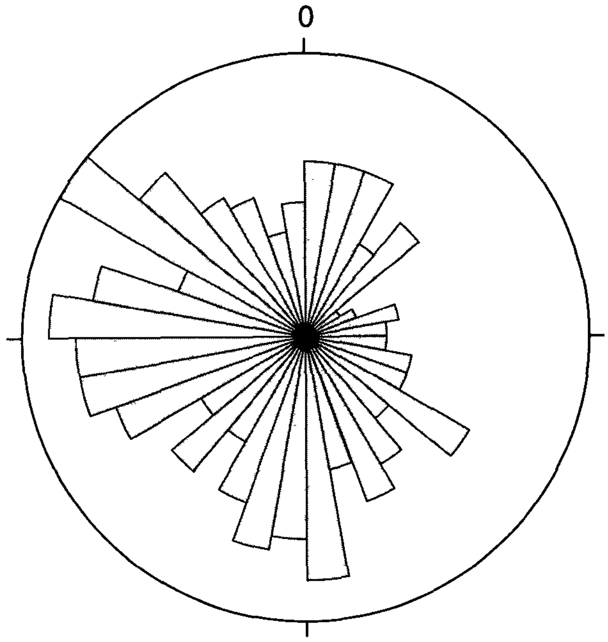

Rose diagram showing frequency of observed fracture dip direction, in 10° classes.

Figure 5. Orientation and distribution of all fractures observed on acoustic-televiewer logs from bedrock wells, Eastern Surplus Superfund Site, Meddybemps, Maine.

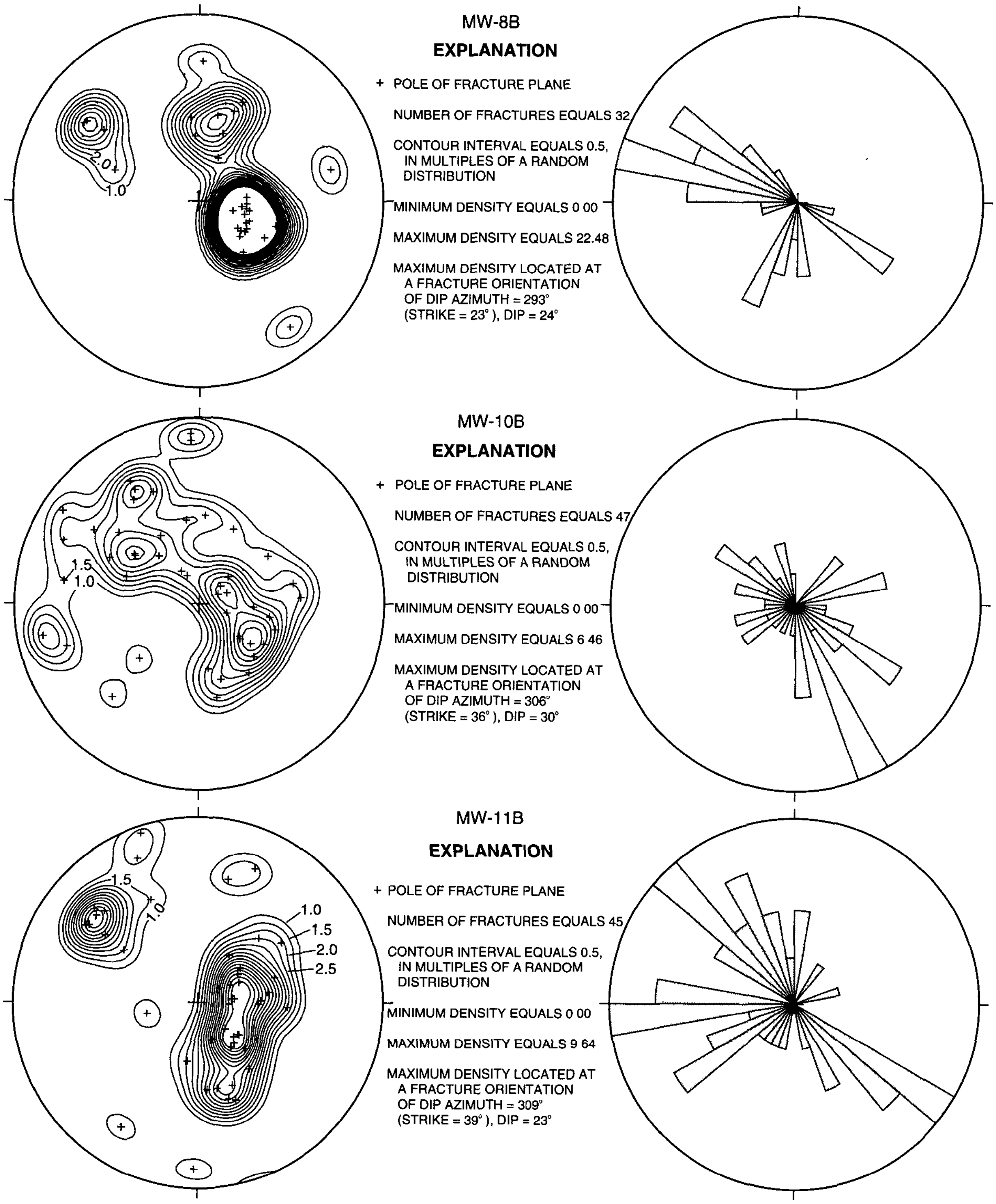

Lower-hemisphere, equal-area stereonet plots of poles to fracture planes and contour plot of relative orientation distribution density of fractures.

Rose diagrams showing probable frequency of fracture dip direction, in 10° classes.

Figure 6. Orientation and distribution of all fractures observed on acoustic-televiewer logs of individual bedrock wells, Eastern Surplus Superfund Site, Meddybemps, Maine.

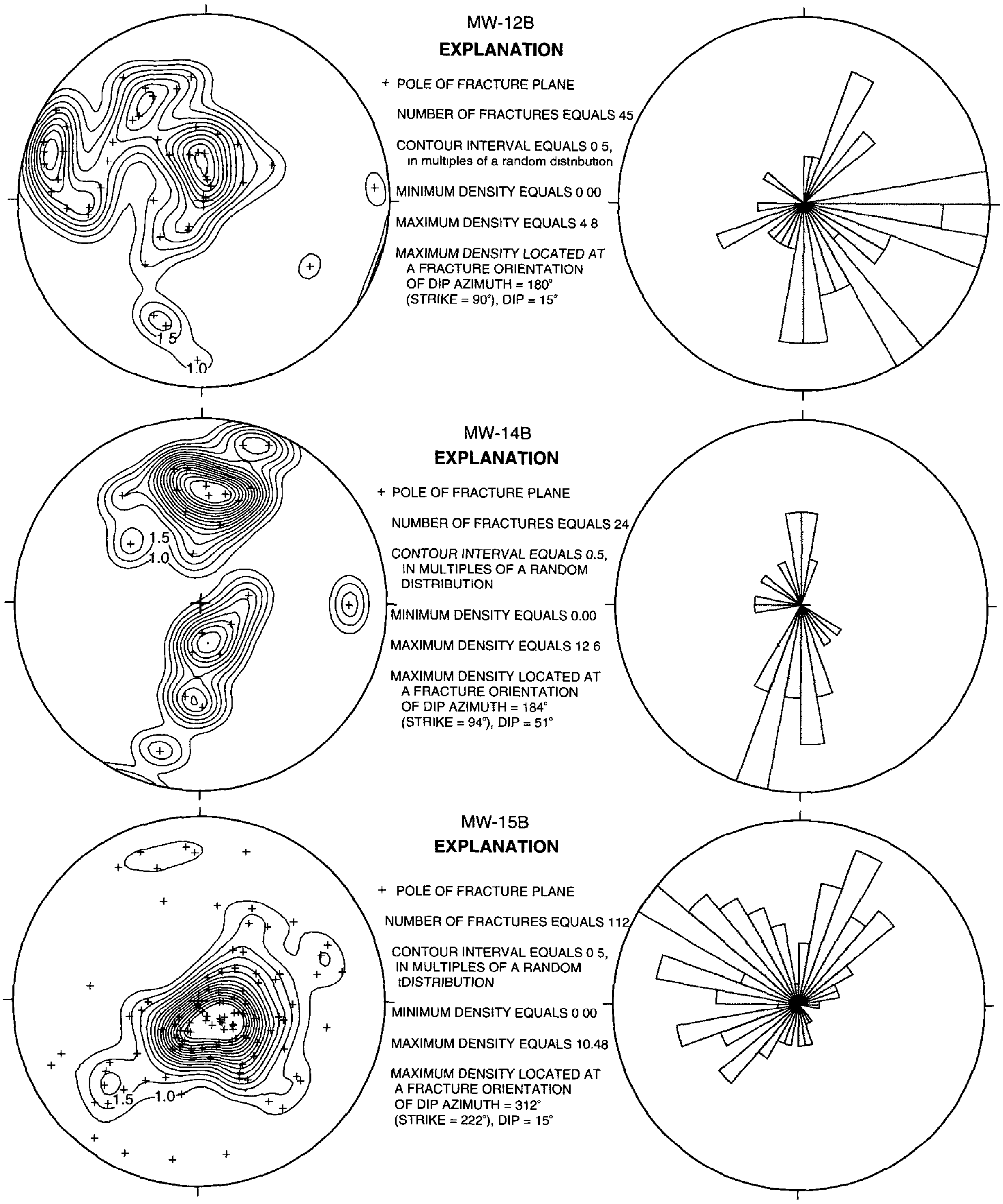

Lower-hemisphere, equal-area stereonet plots of poles to fracture planes and contour plot of relative orientation distribution density of fractures.

Rose diagrams showing probable frequency of fracture dip direction, in 10° classes.

Figure 6. Orientation and distribution of all fractures observed on acoustic-televiewer logs of individual bedrock wells, Eastern Surplus Superfund Site, Meddybemps, Maine—*Continued.*

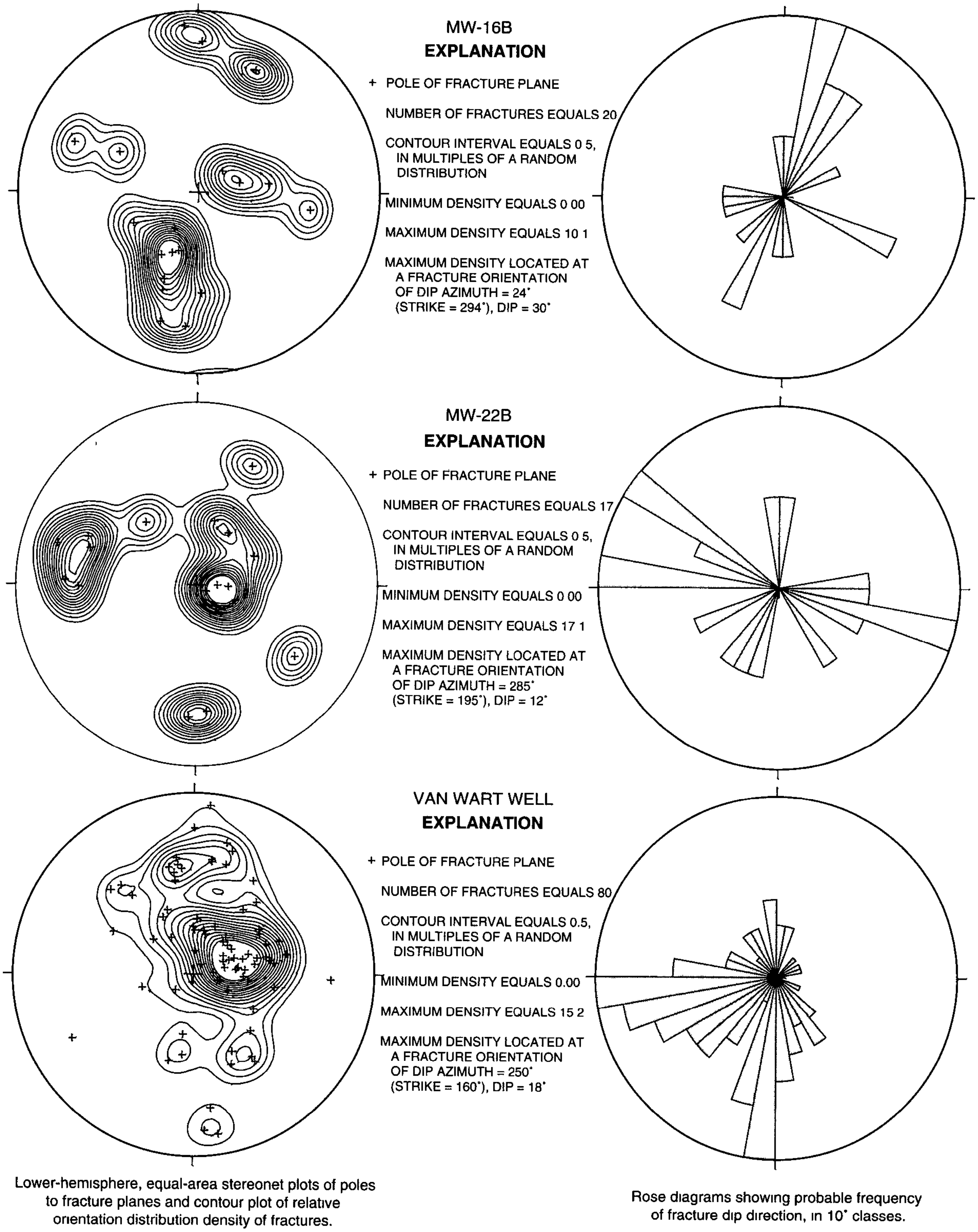

Figure 6. Orientation and distribution of all fractures observed on acoustic-televiewer logs of individual bedrock wells, Eastern Surplus Superfund Site, Meddybemps, Maine—*Continued.*

Single-Hole Directional Radar

The radar records from eight wells (no usable data from the Van Wart well) indicate that radar-wave penetration into the bedrock averaged about 25 ft and ranged from 0 to 50 ft. Radar velocity ranged from 0.26 to 0.32 ft/ns. Calculated dielectric permittivity (Beres and Haeni, 1991) of the crystalline rock ranged from 9.4 to 14.2, which is higher than typically reported for a wet granite (Ulriksen, 1982; Markt, 1988) and indicates relatively conductive materials. The calculated resolution of the radar record (the degree to which individual fractures can be detected) averages about 2.4 ft (Sheriff, 1984; Trabant, 1984). Applying the average radar-wave velocity and data from the radar records, the location and orientation of each radar reflector (fracture or fracture zone) was determined. A total of 224 fractures were identified. The orientation and distribution of fracture density for all the fractures identified from the single-hole directional radar records is shown in figure 7. The data indicate a predominant set of low-angle fractures with an average NNE strike (WNW dip azimuth) that ranges from NE counterclockwise to NW (dip azimuths range from NW to SW). The low-angle fracture set has an average dip of about 18°. A high-angle fracture set striking NNE and dipping ESE is clearly indicated, and two high-angle sets striking E-W and dipping N and S, respectively, are weakly indicated.

Integrated Fracture Orientation

An integrated interpretation of all of the data from the various survey methods indicates the presence of three fracture sets:

- a low-angle set striking NNE and dipping WNW;
- a high-angle set striking NNE and dipping ESE; and
- a second high-angle set striking ENE to E (nearly EW) and dipping SSE to S.

The NNE-striking low-angle fractures were observed on televiewer and directional radar logs. Within this low-angle fracture set there is considerable variation in strike and dip azimuth (figs. 5 and 6). Both of the high-angle fracture sets were indicated by outcrop mapping, square-array resistivity, and televiewer surveys. The NNE-striking high-angle fractures are either vertical (outcrop data) or high angle (televiewer and directional radar data). The vertical NNW-striking fracture set observed on outcrops is weakly indicated by some of the square-array results and is not listed as a major fracture set. A summary of the fracture sets determined by the various surveying methods is listed in table 2.

Table 2. Summary of fracture type and orientation determined by four methods of observation, Meddybemps, Maine

[Azimuths relative to True North; °, degrees; Low-angle fractures, dip equals from 0 to 45 degrees; High-angle fractures, dip equals 45 to 90 degrees]

Method of observation	Fracture type and orientation			
	High-angle fractures		Low-angle fractures	
	Strike	Dip and dip azimuth	Strike	Dip and dip azimuth
Outcrop Mapping	NNW ENE to E–WSW to W	90° (vertical) 75–80° SSE to S	Horizontal and very low-angle fractures observed. Orientation not measured.	
Square-Array Resistivity	NNE–SSW NE–SW NE–SW E–W	Not detected by this method	Not detected by this method	
Acoustic Televiewer	NNE–SSW ENE–WSW	75° ESE 75° SSE	NNE–SSW	18° WNW
Directional Radar	NNE–SSW E–W E–W	60° ESE 70° N 70° S	NNE–SSW	18° WNW

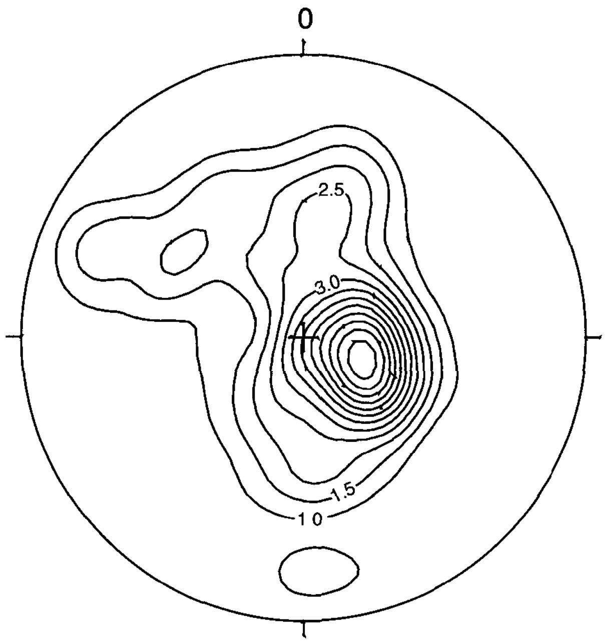

Lower-hemisphere, equal-area stereonet plot of poles to fracture planes and contour plot of relative orientation distribution density of fractures.

EXPLANATION

NUMBER OF FRACTURES EQUALS 224

CONTOUR INTERVAL EQUALS 0.5, IN MULTIPLES OF A RANDOM DISTRIBUTION

MINIMUM DENSITY EQUALS 0.00

MAXIMUM DENSITY EQUALS 6.91

MAXIMUM DENSITY LOCATED AT A FRACTURE ORIENTATION OF DIP AZIMUTH = 290° (STRIKE = 208°), DIP = 18°

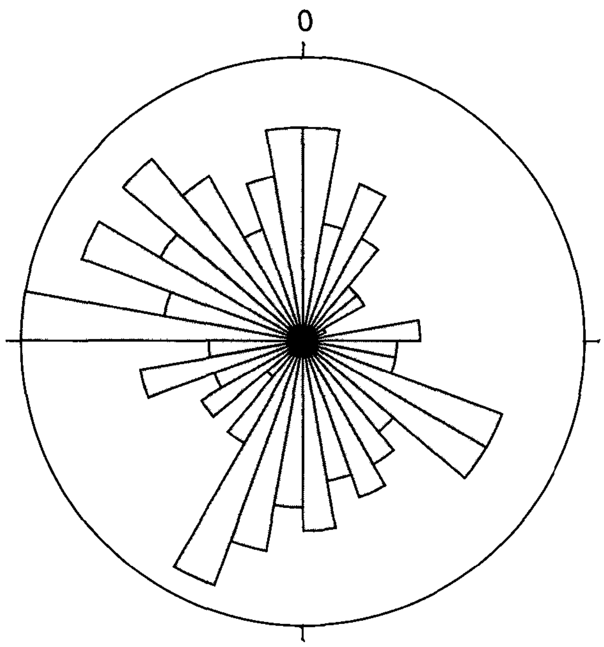

Rose diagram showing probable frequency of fracture dip direction, in 10° classes.

Figure 7. Orientation and distribution of all fractures identified on single-hole directional radar records from bedrock wells, Eastern Surplus Superfund Site, Meddybemps, Maine.

CORRECTION OF FRACTURE DENSITY

The relative abundance of observed fractures with different orientations is partially related to biases associated with the orientation of the field observations. Examination of fractures on horizontal or low-relief outcrops has a higher probability of detecting vertical and high-angle fractures than detecting horizontal fractures. Conversely, vertical boreholes have a high probability of intersecting horizontal fractures and almost zero probability of intersecting a vertical fracture. To account for this sampling bias, a correction based on the orientation of the scan line used to sample fracture orientation (90° for vertical boreholes), and the dip angle of the observed fracture may be applied to a fracture population to determine the probable density (numbers) of fractures actually present. The probable abundance of fractures in a set would be equivalent to the number of fractures intersected by a well drilled normal to their planes. The number of fractures in any equal-area segment (an area bounded by a small range of strike and dip) is multiplied by the inverse of the cosine of the dip angle (Terzaghi, 1965) to determine the probable number of fractures present at the indicated strike and dip. This method has been used in several recent fracture studies (Barton and Zoback, 1992; Morin and others, 1997).

A probability correction was done with the cumulative televiewer fracture-population data from nine wells. The resulting lower-hemisphere equal-area contour plot of fracture density and rose diagrams of fracture dip azimuth are shown in figure 8. The three primary fracture sets are still defined, but the corrected plot indicates that steeply dipping fractures are probably significantly more numerous than observed in boreholes (fig. 5). A larger population of high-angle fractures than was observed on the televiewer record is supported by the radar data, which indicate more high-angle fractures (reflectors) than the televiewer records. The radar logs sampled a much larger horizontal distance than the televiewer (0.5 ft for the televiewer and an average of 50 ft for the radar) in each well. Fractures that were detected by the directional radar but not detected by the televiewer are shown in figure 9. The fractures shown on this figure either do not intersect the surveyed wells or intersect the planes of the wells above or below the open sections of the wells.

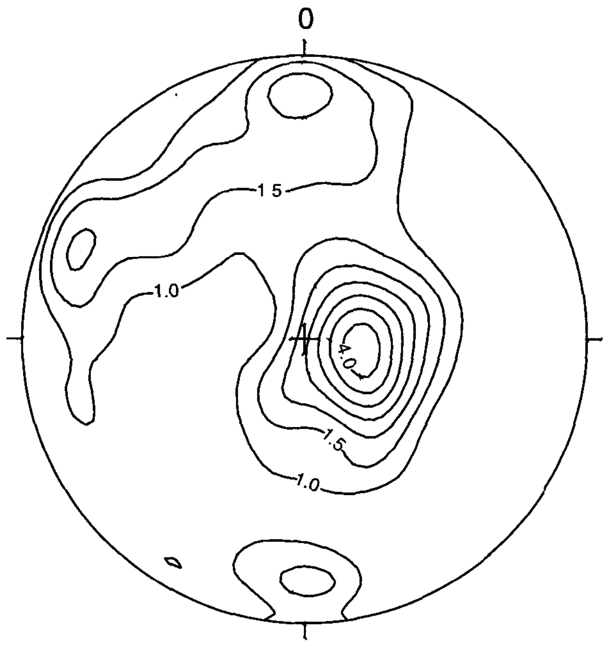

Lower-hemisphere, equal-area stereonet contour plot of probable relative orientation distribution density of fractures.

EXPLANATION

NUMBER OF FRACTURES EQUALS 421

CONTOUR INTERVAL EQUALS 0.5,
IN MULTIPLES OF A RANDOM DISTRIBUTION

MINIMUM DENSITY EQUALS 0.00

MAXIMUM DENSITY EQUALS 4.3

MAXIMUM DENSITY LOCATED AT
A FRACTURE ORIENTATION
OF DIP AZIMUTH = 280°
(STRIKE = 190°), DIP = 18°

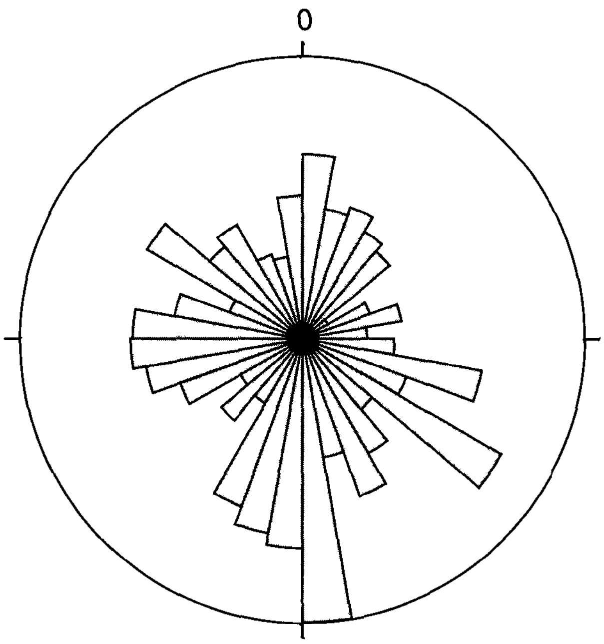

Rose diagram showing probable frequency of fracture dip direction, in 10° classes.

Figure 8. Orientation and probable density distribution of all fractures, Eastern Surplus Superfund Site, Meddybemps, Maine.

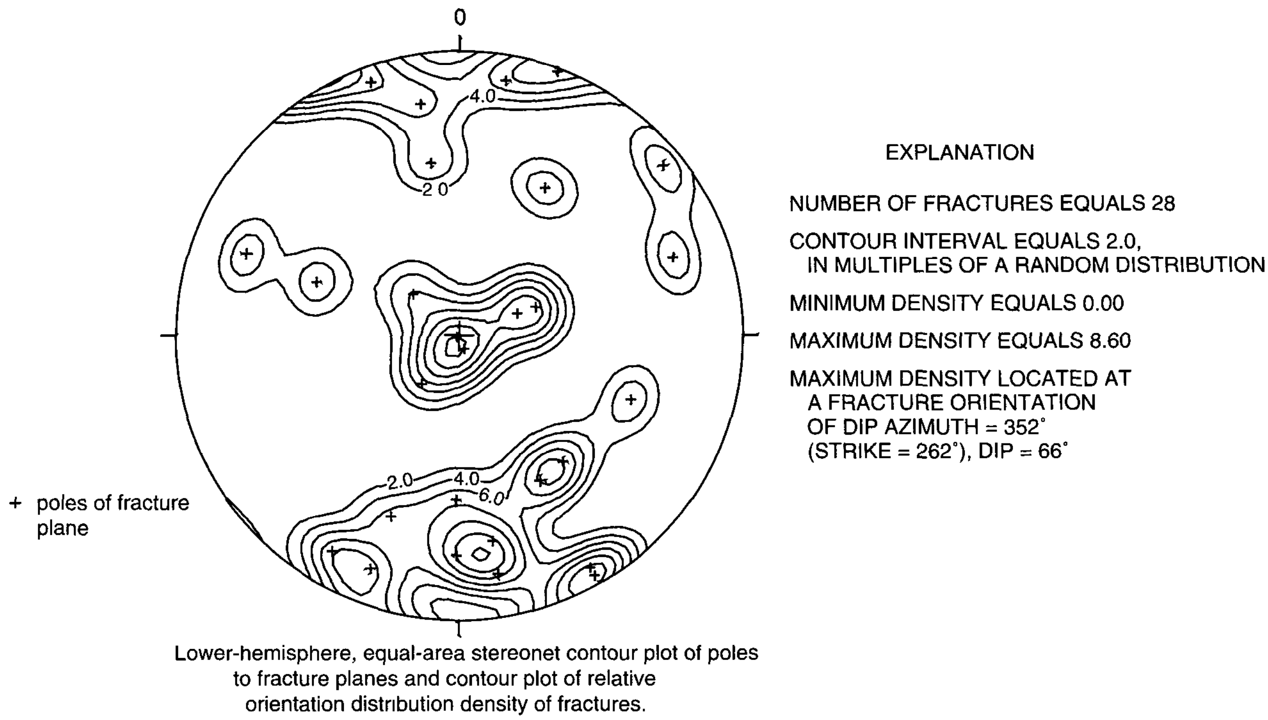

Figure 9. Orientation and distribution of fractures that were detected only by single-hole directional radar surveys, Eastern Surplus Superfund Site, Meddybemps, Maine.

WATER-YIELDING FRACTURES

This section describes the orientation, distribution, probable spacing, and estimated hydraulic properties of water-yielding fractures detected at the study site.

Orientation and Distribution

Permeable fractures were identified by combining the results of flowmeter logging (Lyford and others, 1998) with the fracture data from the acoustic televiewer logs. Most of the flowmeter logging was done before the televiewer logging, and, thus, the depth of discrete fractures was unknown at the time when flowmeter logging was done. Flowmeter logging generally identified small (1- to 5-foot) intervals of borehole that yielded water to the borehole under static and (or) pumping conditions. Televiewer logs were examined to determine the fracture contributing water within each water-yielding interval. In cases where more than one fracture occurred in the water-yielding zone or where fractures intersected, all the fractures in the zone were designated as yielding. Supplemental flowmeter logging done in some wells at small intervals within these water-yielding zones has improved the identification of discrete water-yielding fractures. The distribution and orientation of the water-yielding fractures are shown in figure 10 and are listed in table 3. In general, the water-yielding fractures fall within the three main fracture sets identified for the total fracture population (figs. 5 and 8). However, in contrast to the total fracture population, most of the water-yielding fractures dip southerly. Most of the high-angle water-yielding fractures strike NNE or ENE and dip ESE or SSE. The low-angle water-yielding fractures generally strike NNE to WNW and dip WNW to SSW. The fracture densities of the yielding fractures were corrected based on the Terzaghi (1965) method described previously. The relative density of fractures that are probably present at the site is shown in figure 11.

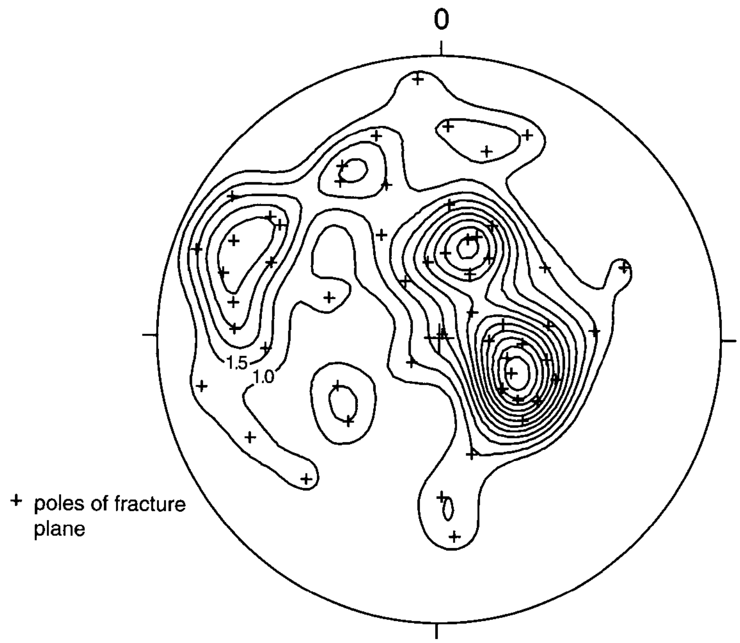

EXPLANATION

NUMBER OF FRACTURES EQUALS 56

CONTOUR INTERVAL EQUALS 0.5, IN MULTIPLES OF A RANDOM DISTRIBUTION

MINIMUM DENSITY EQUALS 0.00

MAXIMUM DENSITY EQUALS 6.9

MAXIMUM DENSITY LOCATED AT A FRACTURE ORIENTATION OF DIP AZIMUTH = 293° (STRIKE = 203°), DIP = 66°

Lower-hemisphere, equal-area stereonet plot of poles to fracture planes and contour plot of relative orientation distribution density of fractures.

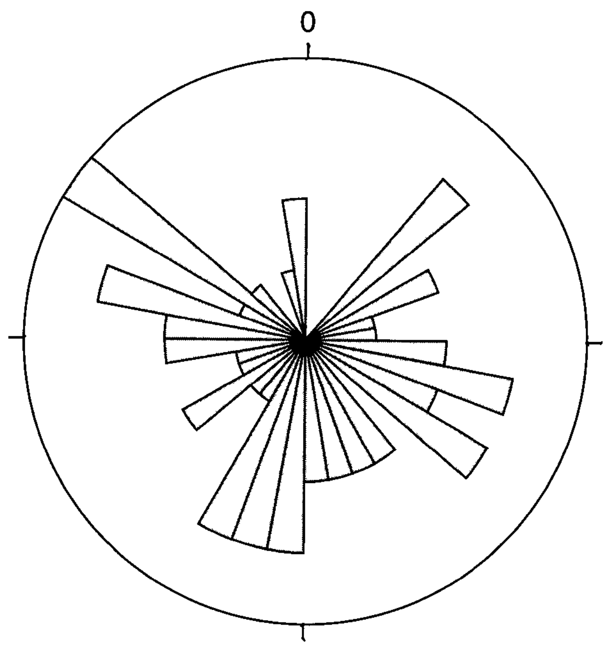

Rose diagram showing probable frequency of fracture dip direction, in 10° classes.

Figure 10. Orientation and distribution of water-yielding fractures interpreted from televiewer and flowmeter logs of bedrock wells, Eastern Surplus Superfund Site, Meddybemps, Maine.

Table 3. Orientation and estimated hydraulic properties of water-yielding fractures in bedrock wells, Eastern Surplus Superfund site, Meddybemps, Maine

[All depths in feet below indicated datum. Azimuth in degrees relative to true north. Shaded areas indicate intersecting fractures or fracture zones. Total estimated apparent transmissivity for each well is average from Lyford and others, U.S. Geological Survey, written commun., 1998. No, number; ft, foot; ft^2/d, foot squared per day; --, no data; >, actual value is greater than value shown; <, actual value is less than value shown; *, probable yielding fracture in fracture zone or where fractures intersect]

Well No. or name	Depth below top of casing	Depth below land surface	Strike azimuth (degrees)	Dip azimuth (degrees)	Dip (degrees)	Estimated apparent trans-missivity (ft^2/d)	Remarks
MW-8B	31.5–32.5	31.2–32.2	92.0	182.0	63.9		
	31.9–32.1	31.6–31.8	205.3	295.3	23.1	0.07	
	58.7–58.9	58.4–58.6	115.1	205.1	20.4		
	59.4–59.7	59.1–59.4	109.9	199.9	31.3	.11	
	76.9–78.0	76.6–77.7	35.0	125.0	62.5	.02	
Well total						0.2	
MW-10B	28.0–28.5	26.6–27.1	--	--	38.4		
	28.0–28.9	26.6–27.5	--	--	59.6	2.14	
	33.7–34.0	32.3–32.6	224.5	314.5	34.4	3.98	
	35.1–35.4	33.7–34.0	211.5	301.5	33.7	.18	
	36.2–36.4	34.8–35.0	218.9	308.9	22.7	.52	
	39.6–40.1	38.2–38.7	177.1	267.1	45.7	.15	
	45.9–46.3	44.5–44.9	253.9	343.9	34.7	.52	
	52.0–53.5	50.6–52.1	24.7	114.7	69.4		
	54.5–56.9	53.1–55.5	33.3	123.3	76.6		
	57.5–57.1	56.1–55.7	215.5	305.5	28.5	.52	
	63.1–63.4	51.7–62.0	190.9	280.9	31.9	.31	
	64.8–65.2	63.4–63.8	199.0	289.0	35.7		
	68.1–68.5	66.7–67.1	146.1	236.1	37.0		
	68.2–69.0	66.8–67.6	313.1	43.1	58.0	.43	
	70.7–71.5	69.3–70.1	57.2	147.2	54.0	.12	
	74.5–75.5	73.1–74.1	34.6	124.6	58.3		
	76.5–77.6	75.1–76.2	9.1	99.1	63.2		
	78.4–78.8	77.0–77.4	115.3	205.3	36.3	1.77	
	79.1–79.5	77.7–78.1	19.3	109.3	34.2		
	81.5–81.9	80.1–80.5	317.3	47.3	36.2	.09	
	83.2–83.5	81.8–82.1	60.0	150.0	34.2	.30	
	96.2–96.4	94.8–95.0	184.4	274.4	23.9		
	97.0–99.2	95.6–97.8	348.6	78.6	74.8	.06	
	104.3–104.4	102.9–103.0	141.7	231.7	12.4	.09	
	112.7–113.1	111.3–111.7	94.0	184.0	38.7		
	113.0–113.9	111.6–112.5	60.2	150.2	58.5	.30	
Well total						11.5	

Table 3. Orientation and estimated hydraulic properties of water-yielding fractures in bedrock wells, Eastern Surplus Superfund site, Meddybemps, Maine—*Continued*

Well No. or name	Depth below top of casing	Depth below land surface	Strike azimuth (degrees)	Dip azimuth (degrees)	Dip (degrees)	Estimated apparent trans-missivity (ft^2/d)	Remarks
MW-11B	36.0–40.0	35.1–39.1	--	--	--	16.2	fracture orientation unknown
	75.5–76.2	74.6–75.3	103.7	193.7	57.5	5.4	
	79.4–80.6	78.5–79.7	113.0	193.7	57.5	64.8	
	130.0–130.2	129.1–129.3	218.1	308.1	23.3	3.6	
Well total						90	
MW-12B	33.2–33.7	32.0–32.5	355.9	85.9	51.7	.16	
	36.3–36.3	35.1–35.1	131.3	221.3	1.2		
	*36.7–40.0	35.5–38.8	19.4	109.4	80.7	.14	
Well total						0.3	
MW-14B	16.0–16.5	14.4–14.9	268.5	358.5	46.7	19.5	
	28.8–29.0	27.2–27.4	81.1	171.1	22.2	6.5	
Well total						26	
MW-15B	77.1–77.3	76.0–76.2	196.4	286.4	20.3	.04	
	*94.7–95.7	93.6–94.6	158.9	248.9	59.6		
	95.9–97.0	94.8–95.9	72.2	162.2	63.8		
	97.6–98.2	96.5–97.1	70.3	160.3	47.7	.06	
Well total						0.1	
MW-16B	48.8–49.1	47.1–47.4	173.1	263.1	32.0	.14	
	68.7–69.0	67.0–67.3	334.3	64.3	32.7		
	69.2–69.4	67.5–67.7	167.5	257.5	18.8	.01	
	100.4–103.8	98.7–102.1	84.9	174.9	80.0	.05	
Well total						0.2	
MW-22B	30.6–31.3	28.7–29.4	23.6	113.6	54.9		
	31.5–32.8	29.6–30.9	16.2	106.2	68.8	382	
	35.9–36.2	34.0–34.3	121.8	211.8	27.1	6.5	
	37.0–37.3	35.1–35.4	105.7	195.7	29.6	8.3	
	43.7–43.8	41.8–41.9	183.5	273.5	14.4		
	43.4–44.2	41.5–42.3	265.1	355.1	59.4		
	44.2–45.2	42.3–43.3	1.9	91.9	61.7	16.5	
	>46.5	>44.6				1.7	
Well total						415	
Van Wart	91.8–91.9	90.4–90.5	318.1	48.1	10.6	5.33	
	94.4–94.6	93.0–93.2	58.5	148.5	18.9		
	95.0–96.1	93.6–94.7	331.9	61.9	64.8	6.40	
	97.7–97.9	96.3–96.5	93.6	183.6	24.6	.26	
Well total						12.0	

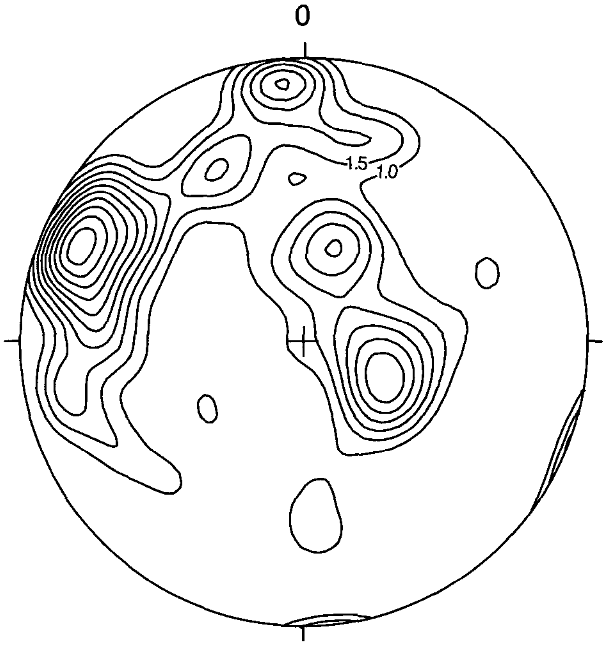

Lower-hemisphere, equal-area stereonet contour plot of probable relative orientation distribution density of fractures.

EXPLANATION

NUMBER OF FRACTURES EQUALS 56

CONTOUR INTERVAL EQUALS 0.5, IN MULTIPLES OF A RANDOM DISTRIBUTION

DENSITY CALCULATED USING A WEIGHTING FACTOR OF 1/COS OF DIP

MINIMUM DENSITY EQUALS 0.00

MAXIMUM DENSITY EQUALS 5.8

MAXIMUM DENSITY LOCATED AT A FRACTURE ORIENTATION OF DIP AZIMUTH = 113° (STRIKE = 23°), DIP = 75°

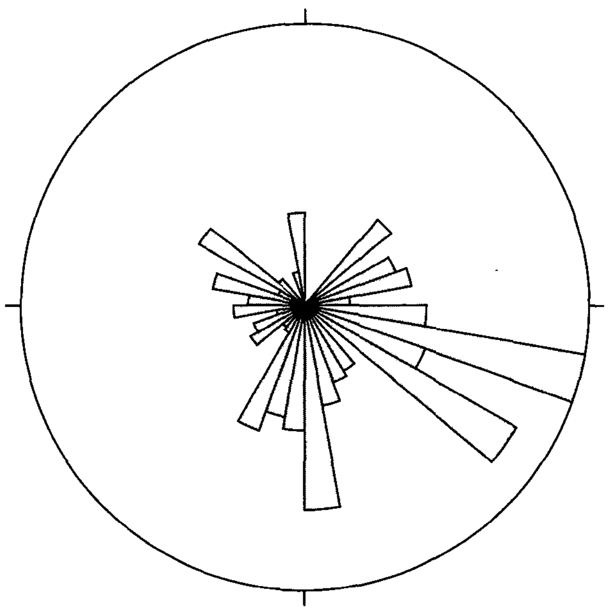

Rose diagram showing probable frequency of fracture dip direction, in 10° classes.

Figure 11. Orientation and probably density distribution of water-yielding fractures, Eastern Surplus Superfund Site, Meddybemps, Maine.

On the basis of the data and a correction applied to account for sampling-orientation bias, the spacing and orientation of water-yielding fractures believed to be present at the Eastern Surplus area were estimated. Statistically, the average spacing (normal to the fracture planes) is estimated to be 30 ft for the low-angle fractures; 27 ft for the NNE-striking, ESE-dipping, high-angle fractures; and 43 ft for the ENE-striking, SSE-dipping high-angle fractures. However, the observed spacing of observed fractures is nonuniform. Some miscellaneous water-yielding high-angle fractures that are not in the main fracture groups are present and probably have an average spacing of 60 ft.

Hydraulic Characteristics

Flowmeter data, which provided the percentage of total well yield produced from each water-yielding fracture or fracture zone during the flowmeter testing, was combined with total apparent fracture transmissivity of each well determined by hydraulic testing (F.P. Lyford and others, U.S. Geological Survey, written commun., 1998) to estimate the apparent transmissivity of each fracture or fracture zone. The estimated transmissivities are listed in table 3. Median apparent transmissivity of individual fractures or fracture zones was 0.3 ft^2/d. Apparent fracture transmissivity ranged from 0.01 to 382 ft^2/d, but 95 percent of the fractures or fracture zones had an apparent transmissivity of 19.5 ft^2/d or less. The largest apparent fracture transmissivity (382 ft^2/d) was associated with a shallow high-angle fracture zone in well MW-22B. Aquifer-test results (F.P. Lyford and others, 1999) indicate that this zone may be hydraulically connected to coarse-grained unconsolidated material that overlies bedrock at this location. The largest apparent fracture transmissivity associated with a single fracture (58 ft^2/d) is in well MW-11B (fig. 2). The hydraulic properties of this high-angle fracture and its location and orientation relative to wells MW-10B and MW-11B, which are separated by more than 200 ft, are probably the reason for the good hydraulic connection observed between these two wells during aquifer testing (F.P. Lyford and others, 1999).

SUMMARY AND CONCLUSIONS

In 1997–98 the USGS, in cooperation with the USEPA, used four geophysical methods to determine fracture orientation in the crystalline bedrock that underlies the Eastern Surplus Superfund Site and adjacent areas in Meddybemps, Maine. The fracture information can be used to assess ground-water and contaminant transport at the site. Azimuthal square-array resistivity surveys were done at 3 sites, borehole-acoustic televiewer and borehole-video logs were collected in 10 wells, and single-hole directional radar surveys in 9 wells.

Azimuthal square-array resistivity data from three sites indicated that the primary high-angle fractures have a generally NE strike. At site 3, the data for depths greater than 42 ft indicated that the high-angle fracture strike shifted to east.

Borehole televiewer data from nine wells indicate the presence of three primary fracture sets, one low-angle set (< 45° dip) and two high-angle sets (> 45° dip). The low-angle fractures strike generally NNE and dip 20° to the WNW. The two high-angle fracture sets strike generally NNE and ENE and dip ESE and SSE, respectively. Observed fracture orientation and density differ considerably from well to well, but the three fracture sets were observed in most data plots from individual wells.

Single-hole directional radar data indicate two primary fracture sets: a low-angle fracture set striking NNE and dipping WNW, and a high-angle fracture set striking NNE and dipping ESE. Two additional high-angle fracture sets are defined weakly, one striking E-W and dipping N; and a second striking E-W and dipping S.

Integrated results from square-array resistivity, televiewer, single-hole directional radar surveys, and previous outcrop mapping indicate the presence of three primary fracture sets. A low-angle fracture set strikes NNE and dips WNW. Two high-angle fracture sets strike NNE and ENE and dip ESE and SSE.

The total number of fractures with different orientations observed with methods used in this study are biased because of the orientation of the field observations. Fracture-population data were adjusted to determine the probable number of fractures present at the site. The corrected data indicate that the high-angle fractures are probably much more numerous than observed in the boreholes.

The orientation and distribution of water-yielding fracture sets were identified by combining the fracture data from this study with the results of borehole-flowmeter logging from a previous study. In general, water-yielding fracture sets correspond to the same three fracture sets as were observed for the total fracture population. In contrast to the total fracture population, most of the water-yielding fractures dip southerly. Most of the low-angle fractures strike generally from NNE to WNW and dip WNW to SSW. The probable average spacing (normal to the fracture plane) between water-yielding fractures in the three fracture sets is estimated to be 30 ft for the low-angle fractures; 27 ft for the NNE-striking, ESE-dipping high-angle fractures; and 43 ft for the ENE-striking and SSE-dipping high-angle fractures. Spacing between water-yielding fractures and fracture sets is variable.

The median estimated apparent transmissivity of individual fractures or fracture zones intersecting bedrock wells in the study area was 0.3 ft^2/d and ranged from 0.01 to 382 ft^2/d: 95 percent of the fractures or fracture zones had an apparent transmissivity of 19.5 ft^2/d or less. The largest apparent transmissivity associated with a single fracture (58 ft^2/d) is in well MW-11B. This high-angle fracture is probably responsible for the good hydraulic connection observed between well MW-11B and well MW-10B during aquifer testing.

The orientation, spacing, and hydraulic properties of water-yielding bedrock fractures identified by this study can be used to help determine recharge, flow, and discharge of ground water and contaminants. High-angle fractures provide vertical pathways for ground water to enter the bedrock, interconnections between low-angle fractures, and, subsequently, pathways for flow within the bedrock along fracture planes. Low-angle fractures may allow horizontal ground-water flow in all directions. The orientation of fracturing and the hydraulic properties of each fracture set will strongly affect changes in ground-water flow under stress (pumping) conditions.

REFERENCES

Barton, C.A., and Zoback, M.D., 1992, Self-similar distribution and properties of macroscopic fractures at depth in crystalline rock in the Cajon Pass Scientific Drill Hole: Journal of Geophysical Research, v. 97, p. 5181–5200.

Beres, Milan, Jr., and Haeni, F.P., 1991, Application of ground-penetrating-radar methods in hydrologic studies: Ground Water, v. 29, no. 3, p. 375–386.

Habberjam, G.M., 1972, The effect of anisotropy on square array resistivity measurements: Geophysical Prospecting, v. 20, p. 249–266.

___ 1975, Apparent resistivity, anisotropy and strike measurements: Geophysical Prospecting, v. 23, p. 211–247.

Hansen, B.P. and Lane, J.W., Jr., 1995, Use of surface and borehole geophysical surveys to determine fracture orientation and other site characteristics in crystalline bedrock terrain, Millville and Uxbridge, Massachusetts: U.S. Geological Survey Water-Resources Investigations Report 95-4121, 25 p.

Keys, W.S., 1990, Borehole geophysics applied to ground-water investigations: U.S. Geological Survey Techniques of Water-Resources Investigations, book 2, chap. E2, 150 p.

Kierstein, R.A., 1983, True location and orientation of fractures logged with the acoustic televiewer: U.S. Geological Survey Water-Resources Investigations Report 83-4275, 71 p.

Lane, J.W., Jr., Haeni, F.P., and Watson, W.M., 1995, Use of square-array direct-current resistivity method to detect fractures in crystalline bedrock in New Hampshire: Ground Water, v. 33, no. 3, p. 476–485.

Lane, J.W., Jr., Haeni, F.P., and Williams, J.H., 1994, Detection of bedrock fractures and lithologic changes using borehole radar at selected sites, *in* Fifth International Conference on Ground-Penetrating Radar, Kitchener, Ontario, Canada, June 12–16, 1993, Proceedings: Waterloo, Ont., Can., Waterloo Centre for Groundwater Research, p. 577–591.

Lau, J.S.O., 1983, The determination of true orientation of fractures in rock cores: Canadian Geotechnical Journal, v. 20, no. 3, p. 221–227.

Lieblich, D.A., Haeni, F.P., and Cromwell, R.E., 1992a, Integrated use of surface-geophysical methods to indicate subsurface fractures at Tibbetts Road, Barrington, New Hampshire: U.S. Geological Survey Water-Resources Investigations Report 92-4012, 33 p.

Lieblich, D.A., Lane, J.W., Jr., and Haeni, F.P., 1991, Results of integrated surface-geophysical studies for shallow subsurface fracture detection at three New Hampshire sites, *in* Expanded Abstracts with Biographies, SEG 61st Annual International Meeting, Houston, Texas, November 10–14, 1991: Houston, Tex., Society of Exploration Geophysicists, p. 553–556.

Lieblich, D.A., Haeni, F.P., and Lane, J.W., Jr., 1992b, Integrated use of surface-geophysical methods to indicate subsurface fractures at Milford, New Hampshire: U.S. Geological Survey Water-Resources Investigations Report 92-4056, 38 p.

Ludman, Allan, 1982, Bedrock geology of the Fredericton 2-degree quadrangle, Maine: Maine Geological Survey, Open-File No. 82-30, 16 p., scale 1:250,000.

Ludman, Allan, and Hill, Malcolm, 1990, Bedrock geology of the Calais 15′ quadrangle, eastern Maine: Maine Geological Survey Open-File No. 90-27, 32 p., scale 1:62,500.

Lyford, F.P., Garabedian, S.P., and Hansen, B.P., 1999, Estimated hydraulic properties for the surficial- and bedrock-aquifer system, Meddybemps, Maine: U.S. Geological Survey Open-File Report 99-199, ___ p.

Lyford, F.P., Stone J.R., Nielsen, J.P., and Hansen, B.P., 1998, Geohydrology and ground-water quality, Eastern Surplus Superfund Site, Meddybemps, Maine: U.S. Geological Survey Water-Resources Investigations Report 98-4174, 68 p.

Markt, George, 1988, Subsurface characterization of hazardous waste sites using ground-penetrating radar, *in* Second International Symposium on Geotechnical Applications of Ground-Penetrating Radar, March 6–10, 1988, Proceedings: 41 p.

Morin, R.H., Carleton, G.B., and Poirier, Stephane, 1997, Fractured-aquifer hydrology from geophysical logs; the Passaic Formation, New Jersey: Ground Water, v. 35, no. 2, p. 328–338.

Osberg, P.H., Hussey, A.M., and Boone, G.M. (eds.), 1985, Bedrock geologic map of Maine: Maine Geological Survey, scale 1:500,000.

Paillet, F.L., and Ollila, Paul, 1994, Identification, characterization, and analysis of hydraulically conductive fractures in granitic basement rocks, Millville, Massachusetts: U.S. Geological Survey Water-Resources Investigations Report 94-4185, 36 p.

Safko, P.S., and Hickey, J.J., 1992, A preliminary approach to the use of borehole data, including television surveys, for characterizing secondary porosity of carbonate rocks in the Floridan aquifer system: U.S. Geological Survey Water-Resources Investigations Report 91-4168, 70 p.

Sheriff, R.E. 1984, Encyclopedic dictionary of exploration geophysics (2d ed.): Tulsa, Okla., Society of Exploration Geophysics, 323 p.

Terzaghi, R.D., 1965, Sources of error in joint surveys: Geotechnique, v. 15, p. 287–304.

Trabant, P.K., 1984, Applied high-resolution geophysical methods: Boston, International Human Resources Development Corp., 265 p.

Ulriksen, P.F., 1982, Application of impulse radar to civil engineering: Lund, Sweden, Lund University of Technology, Ph.D. Thesis, 179 p.

Zemanek, Joseph, Caldwell, R.L., Glen, E.E., Halcomb, S.V., Norton, L.J., and Strauss, A.J.D., 1969, The borehole televiewer—a new logging concept for fracture location and other types of borehole inspection: Journal of Petroleum Technology, v. 21, no. 6, p. 762–774.